

Novel kinematics from a custodially protected diphoton resonance

Jack H. Collins,^{*} Csaba Csáki,[†] Jeff A. Dror,[‡] and Salvator Lombardo[§]
Department of Physics, LEPP, Cornell University, Ithaca, NY 14853, USA

We study a simple, well-motivated model based on a custodial symmetry which describes the tree-level production of a 750 GeV diphoton resonance from a decay of a singly produced vector-like quark. The model has several novel features. The identification of the resonance as an $SU(2)_R$ triplet provides a symmetry explanation for suppression of its decays to hh , WW , and gg . Moreover, the ratio of the 13 TeV to 8 TeV cross sections can be larger than single production of a 750 GeV resonance, reaching ratios of up to 7 for TeV scale vector-like quark masses. This eliminates any tension between the results from Run I and Run II diphoton searches. Lastly, we study the kinematics of our signal and conclude that the new production mechanism is consistent with available experimental distributions in large regions of parameter space but, depending on the mass of the new vector-like quarks, can be differentiated from the background with more statistics.

I. INTRODUCTION

The recent observation of an excess in the diphoton channel around 750 GeV invariant mass by ATLAS and CMS at $\sqrt{s} = 13$ TeV [1, 2] has generated much interest in models with a heavy scalar resonance, ϕ , that decays to two photons. Most explanations proposed so far are considering loop induced resonance production, typically via heavy vector-like quarks (VLQ) charged under the Standard Model (SM). Otherwise, tree-level decays to SM particles would naturally dominate the branching ratio of ϕ , either leading to a diphoton rate too small to explain the excess or a production rate of two SM particles with large invariant mass that is excluded by existing measurements.

In this paper, we propose a novel tree-level production mechanism where ϕ arises from the decay of a VLQ. The VLQs can be singly produced due to their mixing with the SM quarks, while the resonance is protected by the $SU(2)_L \times SU(2)_R$ custodial symmetry. In order to have significant mixing between the VLQs and the light quarks without modifying the $Zq\bar{q}$ couplings predicted by the SM, we introduce VLQs in a bidoublet representation of the custodial symmetry, while the resonance ϕ is part of a triplet under $SU(2)_R$. The model has several advantages and new features:

- It is one of the few viable examples of tree-level production consistent with the excess signal rate, existing experimental constraints, and the kinematic distributions of the diphoton background events.
- The ratio of production rates between 13 and 8 TeV is different than gluon or quark fusion. Depending on the model the ratio can be as large as about 7 (vs. 4.7 for gluon fusion), eliminating the tension with the 8 TeV diphoton searches.

- The custodial symmetry protects the resonance from the leading one-loop decays to hh , WW , and gg , while allowing decays to $\gamma\gamma$. The suppression of the hh decay is particularly significant since in most models this coupling will arise at tree-level, making it difficult to reconcile with the expectantly large diphoton branching ratio and unobserved hh decays. The $\gamma\gamma$ (as well as ZZ and $Z\gamma$) decay width is nonvanishing due to the explicit breaking of the custodial symmetry from gauging the $U(1)_Y$ subgroup of $SU(2)_R$.
- The custodial symmetry also forbids one-loop gluon fusion production, explaining the dominance of the tree-level production via a decay of a VLQ.

The scenario where ϕ is produced primarily from the decay of singly-produced VLQs has not been considered in the diphoton excess literature, although some authors have considered production of ϕ through a cascade decay of a heavier parent particle (e.g., [3–10]). Furthermore, several authors have pointed out the potential to measure VLQ top or bottom partners decaying to ϕ [11–13]. However, to explain the bulk of the excess signal through a decay of pair-produced top or bottom partners would require couplings at their perturbative limits to achieve large enough $\gamma\gamma$ rate and to explain why the VLQ decay process dominates over gluon fusion [5]. Moreover, pair production of two VLQs per event would give several hard jets in the event in addition to the diphoton, which is inconsistent with the kinematic distributions of events in the excess region. The tree-level production mechanism presented in this paper avoids these problems. Interestingly, it has been pointed out in [14] that a top partner need not be a mass eigenstate but rather could be a mixture of top and charm-like mass eigenstates raising the possibility that the vector-like quarks which mix with light quarks could also play a role in solving the little hierarchy problem.

This paper is organized as follows. In Sec. II, we introduce a motivated model consistent with low energy flavor constraints in which a bidoublet of vector-like quarks with $m_V \gtrsim m_\phi$ mix with the light-SM quarks. In Sec. III

^{*} jhc296@cornell.edu

[†] csaki@cornell.edu

[‡] ajd268@cornell.edu

[§] sdl88@cornell.edu

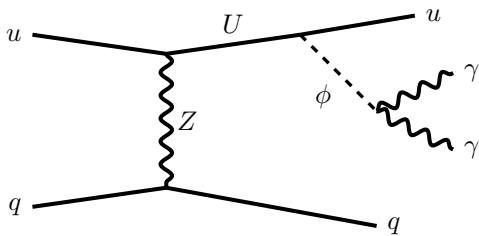


FIG. 1: The dominant production of the diphoton excess from a decaying VLQ (U). In addition to the resonance, there are two additional jets. The p_T of the jets (and hence the visibility of the signal) is strongly dependent on the mass of the VLQ.

we discuss the production and decays of the new particles and find that the model can easily accommodate the current excess in the diphoton data without tension from existing searches, both from the 8 TeV searches sensitive to the 750 GeV resonance as well as searches sensitive to VLQs. Furthermore, we compare the kinematic distributions of our signal and the diphoton background, finding that, depending on the splitting between the VLQ and the scalar, the distributions can be challenging to distinguish without additional data.

II. CUSTODIAL SYMMETRY AND LIGHT QUARK MIXING

In this section, we present a model in which the resonance is a decay product of an electroweak produced VLQ from the dominant t -channel process shown in figure 1. Single production of VLQs requires a large mixing angle between the light quarks and VLQs. One would naively expect such mixing to yield large corrections to the $Zq\bar{q}$ couplings, which are strongly constrained by electroweak precision observables. However, we can protect the Z couplings via the custodial symmetry by using a bidoublet representation V for the VLQs [15]. In addition, we introduce the $SU(2)_R$ triplet, Φ , whose neutral component (which we denote by ϕ) will play the role of the 750 GeV resonance. This model is an example of a custodially symmetric model commonly considered in composite Higgs and extra dimensional models [14, 16–23].

A. Field content and mixing

We organize the fields into irreducible representations of $SU(3)_C \times SU(2)_L \times SU(2)_R \times U(1)_X$ in Table I, where the $SU(2)_R$ is a global symmetry and the fermions are left-handed Weyl spinors. Hypercharge is embedded in $SU(2)_R \times U(1)_X$ as $Y = T_R^3 + X$. The SM quarks are taken to be singlets under $SU(2)_R$ and we represent the Higgs doublet as a bifundamental, $\mathcal{H} = (\epsilon H^*, H)$.

Field	$SU(3)_C$	$SU(2)_L$	$SU(2)_R$	$U(1)_X$
Φ	1	1	3	0
V	3	2	2	+2/3
\bar{V}	$\bar{3}$	2	2	-2/3
\mathcal{H}	1	2	2	0
Q	3	2	1	+1/6
\bar{u}	$\bar{3}$	1	1	-2/3

TABLE I: The representations of relevant fields. The new vector-like quarks are in a single bidoublet V , and the 750 GeV resonance is the neutral component of Φ .

The Higgs and the light quarks have the usual SM assignments. All fermionic fields are left-handed Weyl spinors.

Four VLQs form the bidoublet,

$$V \equiv \begin{pmatrix} U_1 & X \\ D & U_2 \end{pmatrix}, \quad \bar{V} \equiv \begin{pmatrix} \bar{U}_1 & \bar{D} \\ \bar{X} & \bar{U}_2 \end{pmatrix}. \quad (1)$$

The charges of the new quarks are $Q_{U_1} = Q_{U_2} = 2/3$, $Q_D = -1/3$, and $Q_X = 5/3$.

The Lagrangian for the VLQs (not including the terms coupling to the scalar Φ) is

$$\mathcal{L}_{VLQ} = m_V \text{Tr} [\bar{V}V] - \lambda_V \text{Tr} [\mathcal{H}^\dagger V] \bar{u}^{(0)} + h.c., \quad (2)$$

where the (0) superscript denotes the quark fields in the SM mass basis of the up-type sector (the basis of diagonal SM Yukawa couplings). We assume the VLQs only mix with a single generation of right-handed up-type quark, however in appendix A 4 we also consider a different $U(1)_X$ charge for V and the case of mixing with one generation of right-handed down-type quark. Note that we have made an important assumption regarding alignment: the bidoublet V couples to the up-type quark in the mass basis of the SM. This assumption is to avoid low energy flavor constraints from flavor changing neutral currents but is not a crucial ingredient for the collider phenomenology that follows.

The down-type quark masses are unaffected by the new VLQs. One flavor of the up-type quarks can mix significantly with the new VLQs through the off-diagonal mass matrix:

$$\begin{pmatrix} u^{(0)} & U_1 & U_2 \end{pmatrix} \begin{pmatrix} \lambda_u v/\sqrt{2} & 0 & 0 \\ -\lambda_V v/\sqrt{2} & m_V & 0 \\ -\lambda_V v/\sqrt{2} & 0 & m_V \end{pmatrix} \begin{pmatrix} \bar{u}^{(0)} \\ \bar{U}_1 \\ \bar{U}_2 \end{pmatrix} + h.c. \quad (3)$$

where λ_u is the Yukawa of the up-type quark. From here on, we assume the mixing is with the up or charm quark and neglect the up-type quark mass. The mass eigenstates (u , U , and \bar{U}) are related to the gauge eigenstates by:

$$\begin{pmatrix} \bar{u}^{(0)} \\ \bar{U}_1 \\ \bar{U}_2 \end{pmatrix} = \begin{pmatrix} 1 & 0 & 0 \\ 0 & 1/\sqrt{2} & -1/\sqrt{2} \\ 0 & 1/\sqrt{2} & 1/\sqrt{2} \end{pmatrix} \begin{pmatrix} c_\theta & -s_\theta & 0 \\ s_\theta & c_\theta & 0 \\ 0 & 0 & 1 \end{pmatrix} \begin{pmatrix} \bar{u} \\ \tilde{U} \\ \bar{U} \end{pmatrix} \quad (4)$$

$$\begin{pmatrix} u^{(0)} \\ U_1 \\ U_2 \end{pmatrix} = \begin{pmatrix} 1 & 0 & 0 \\ 0 & 1/\sqrt{2} & -1/\sqrt{2} \\ 0 & 1/\sqrt{2} & 1/\sqrt{2} \end{pmatrix} \begin{pmatrix} u \\ \tilde{U} \\ U \end{pmatrix}$$

where $s_\theta \equiv \sin \theta$ and $c_\theta \equiv \cos \theta$ with

$$s_\theta = \frac{\lambda_V v}{m_{U^+}}, \quad (5)$$

where $v \simeq 246$ GeV is the vacuum expectation value of the Higgs, and the masses of the VLQs are $m_{U^-} = m_D = m_\chi = m_V$ and $m_{U^+} = \sqrt{m_V^2 + \lambda_V^2 v^2}$. The down-sector does not experience any mixing, i.e. X and D are mass eigenstates.

The mixing, parameterized by s_θ , leads to couplings between a generation of SM quarks, SM gauge bosons, and the VLQs (derived in more detail in appendix A):

$$\mathcal{L}_{EW} = -\frac{e s_\theta}{2 c_w s_w} Z_\mu \bar{u}^\dagger \bar{\sigma}^\mu \bar{U} - \frac{g s_\theta}{2} W_\mu^- (\bar{u}^\dagger \bar{\sigma}^\mu \bar{D} + \bar{X}^\dagger \bar{\sigma}^\mu \bar{u}) + h.c., \quad (6)$$

where s_w (c_w) is the sine (cosine) of the Weinberg angle and g (e) is the $SU(2)_L$ (QED) coupling constant. If the mixing angle is sufficiently large, these couplings can result in electroweak production of single VLQs (U , D , or X) which can dominate over the VLQ pair production cross section. Notice that only U , which will be responsible for the production of the diphoton resonance, couples to an up-type quark and the Z . \tilde{U} is not produced by electroweak interactions in this model. This is because only the linear combination $\bar{U}_1 + \bar{U}_2$ mixes with the up-type quark, which is a necessary feature for the protection of the $Zq\bar{q}$ coupling in this model.

B. Consequences of a custodial triplet

The 750 GeV diphoton resonance ϕ is embedded in an $SU(2)_R$ triplet scalar Φ as follows.

$$\Phi = \begin{pmatrix} \phi/\sqrt{2} & \phi_+ \\ \phi_- & -\phi/\sqrt{2} \end{pmatrix} \quad (7)$$

This allows for a coupling of Φ to the VLQs of the form

$$\mathcal{L}_\Phi = \sqrt{2} y_\phi \text{Tr} [\bar{V} \Phi V] + h.c. \quad (8)$$

$$= y_\phi \phi (U_1 \bar{U}_1 - U_2 \bar{U}_2 + X \bar{X} - D \bar{D}) + h.c. + \dots \quad (9)$$

$$= y_\phi \phi \left(-s_\theta U \bar{u} - \tilde{U} \bar{U} - c_\theta U \bar{\tilde{U}} + X \bar{X} - D \bar{D} \right) + h.c. + \dots \quad (10)$$

where the ellipses refer to terms involving the charged components of Φ . The relative minus sign between the $U_1 \bar{U}_1$ and $U_2 \bar{U}_2$ terms gives rise to the coupling of ϕ to U and the SM up quark (as opposed to a coupling to \tilde{U}) which is responsible for the production of the resonance.

These interactions will generate couplings of ϕ to SM dibosons, such as gg , WW , hh etc. via triangle diagrams with the VLQs. However, in the limit of exact custodial symmetry, these amplitudes are forbidden. For example, the operator $\Phi G^{\mu\nu, A} G_{\mu\nu}^A$ has no custodially invariant contraction because the gluon field strength tensor G is a custodial singlet. Furthermore, the Higgs coupling to the scalar vanishes since (using $\mathcal{H} \mathcal{H}^\dagger \propto \mathbb{1}$),

$$\text{Tr} [\mathcal{H}^\dagger \Phi \mathcal{H}] \propto \text{Tr} \Phi = 0. \quad (11)$$

In practice, the vanishing of the amplitudes is a consequence of cancellations of the contributions due to different VLQs running in the loop, which contain important relative minus signs as a consequence of the custodial symmetry.

The loop amplitudes for ϕ therefore require the insertion of $SU(2)_R$ violating interactions. The largest such couplings in the SM are the third generation Yukawas, however in the flavor alignment limit these couplings will not directly affect the diphoton resonance sector since we assume mixing is not occurring with the third generation up-type quark. The dominant source of custodial symmetry breaking in this sector will therefore be the embedding of the hypercharge gauge group within the T_3^R generator of $SU(2)_R$, and so it is to be expected that the leading loop amplitude will be that coupling ϕ to hypercharge gauge bosons, $\phi B^{\mu\nu} B_{\mu\nu}$. Indeed, the one-loop contributions to this operator do not cancel among the VLQs due to their differing hypercharges. The other loop amplitudes will be generated at higher order and are suppressed by an additional factor $\sim \alpha/4\pi c_w^2$ compared to their naive sizes. These two-loop contributions can induce a mixing angle between ϕ and the Higgs of order $\sim (v/16\pi^2 m_\phi) (\alpha/4\pi c_w^2)$ (where m_ϕ denotes the mass of the resonance), however this is much too small to induce sizable decays to $t\bar{t}$. Direct couplings of ϕ to the up-type quarks can also arise at two-loops but is suppressed by a Yukawa coupling, making it negligible. We verify the effects of custodial symmetry breaking explicitly in A 3. This custodial protection mechanism generates a natural hierarchy between the decays of the resonance to diphotons and its decays to gg , WW , hh , and also suppresses the gluon fusion production of ϕ .

We now briefly compare this to a scenario in which the diphoton resonance is assumed to be a custodial singlet S with couplings

$$\mathcal{L}_S = y_S S \text{Tr} [\bar{V} V] + h.c. \quad (12)$$

$$= y_S S (U_1 \bar{U}_1 + U_2 \bar{U}_2 + D \bar{D} + X \bar{X}) + h.c. \quad (13)$$

$$= y_S S \left(s_\theta \tilde{U} \bar{u} + U \bar{U} + c_\theta \tilde{U} \bar{\tilde{U}} + D \bar{D} + X \bar{X} \right) + h.c. \quad (14)$$

In this case, the only S -quark-VLQ coupling involves \tilde{U} , which does not couple to SM gauge bosons and therefore cannot be produced via VLQ single production. \tilde{U} is pair-produced and can decay $\tilde{U} \rightarrow Su$, however the rate for pair production is subdominant to electroweak production of U and insufficient to explain the excess. Furthermore, this singlet does not exhibit custodial protection, which is a consequence of the couplings in eq. 13 adding constructively rather than destructively.

III. DIPHOTON CROSS SECTION

Above we presented a model in which ϕ can be produced as a decay product of a singly produced VLQ (we will assume $m_V > m_\phi$ throughout). The dominant production mechanism for the diphoton resonance is depicted in figure 1.¹ In this section, we demonstrate that the $\gamma\gamma$ rate is sufficient to explain the diphoton excess while avoiding constraints from existing VLQ searches and electroweak precision tests. We consider two variations of the model, one where the VLQs mix with the up quark and another with the VLQs mixing with the charm quark.

Since the $\gamma\gamma$ final state arises from a decay chain, the inclusive cross section into $\gamma\gamma$ is given in the narrow width approximation by

$$\sigma_{\gamma\gamma} = \sigma(pp \rightarrow U\bar{u}, \bar{U}u) \times \text{Br}(U \rightarrow \phi u) \times \text{Br}(\phi \rightarrow \gamma\gamma). \quad (15)$$

Each of these contributions has different dependence on the relevant parameters of the model, y_ϕ and s_θ . The production cross section of the VLQs, $\sigma(pp \rightarrow U\bar{u}, \bar{U}u)$, is proportional to s_θ^2 but is independent of y_ϕ .

A. Branching ratios

The complete formulae for the branching ratios of ϕ and U are given in appendix A 2. We summarize the results here. U has two decay channels, $U \rightarrow Zj$ and $U \rightarrow \phi j$ with the dominant decay being Zj . This results in the branching ratio of $U \rightarrow u\phi$ ranging between 1-10%, proportional to y_ϕ^2 and independent of the mixing angle. ϕ has competing decays between a 3-body tree-level decay and loop-induced 2-body decays. The only tree-level decay of ϕ is to $Zu\bar{u}$ through an off-shell U with a rate is proportional to $s_\theta^4 y_\phi^2$, making it highly sensitive to the

¹ Secondary production modes from UZ production, pair production of VLQs, and direct ϕZ production mediated by a VLQ make up 10-30% of inclusive diphoton cross section. We explore the size of different contributions in Sec. IV B, but since the size of the subdominant modes is highly dependent on the detailed parameters of the model, we only include the dominant production when studying the inclusive diphoton rate and kinematics.

	y_ϕ	s_θ
u_R benchmark	0.7	0.1
c_R benchmark	2	0.3

TABLE II: Benchmark points for the up quark and charm quark mixing models. For the u_R model, there are more stringent constraints on the mixing angle though a larger production cross section.

mixing angle. ϕ has additional loop-induced decays into $\gamma\gamma$, $Z\gamma$, and ZZ . These decays arise from gauging hypercharge resulting in the relative ratios,

$$\Gamma_{\gamma\gamma} : \Gamma_{Z\gamma} : \Gamma_{ZZ} = 1 : 2 \tan^2 \theta_w : \tan^4 \theta_w. \quad (16)$$

The loop-induced rates are largely independent of the mixing, proportional to y_ϕ^2 .²

The leading branching ratios of ϕ are shown in figure 2 for a benchmark point relevant in the case of up-mixing with $s_\theta = 0.1$ (left) and charm-mixing with $s_\theta = 0.3$ (right). A couple comments on the choice of benchmark points (displayed in Table II) are in order. First, regarding the size of the mixing angle, we have provided constraints on the allowed mixing angle for electroweak produced VLQs in appendix B, obtained by reinterpreting the constraints from direct LHC searches on light quark composite partner models [14]. For the up-quark mixing, the mixing angle is experimentally constrained to be $s_\theta \lesssim 0.12$, while for charm mixing, the constraints are much weaker with $s_\theta \lesssim 0.5$. Larger mixing angles are allowed for the case of charm mixing since the electroweak production cross section of the VLQs are suppressed by the charm parton distribution function.

B. The inclusive cross section

Depending on the size of mixing, the inclusive cross section for diphoton production scales differently with the mixing angle. There are two distinct regimes, large and small mixing angles. If the mixing angle is large, then the dominant decay of ϕ is through the 3-body decay. In this case the branching ratio into diphotons is $\propto 1/s_\theta^4$ giving an inclusive cross section

$$\sigma_{\gamma\gamma} \propto \frac{y_\phi^2}{s_\theta^2} \quad (\text{large mixing}). \quad (17)$$

² We have checked that non-zero mixing has at most a 10% effect on the loop-induced rates in the region of parameter space we are interested in. Furthermore, these effects will not have any bearing on the size of the $\gamma\gamma$ rate and thus we ignore these effects in our analysis.

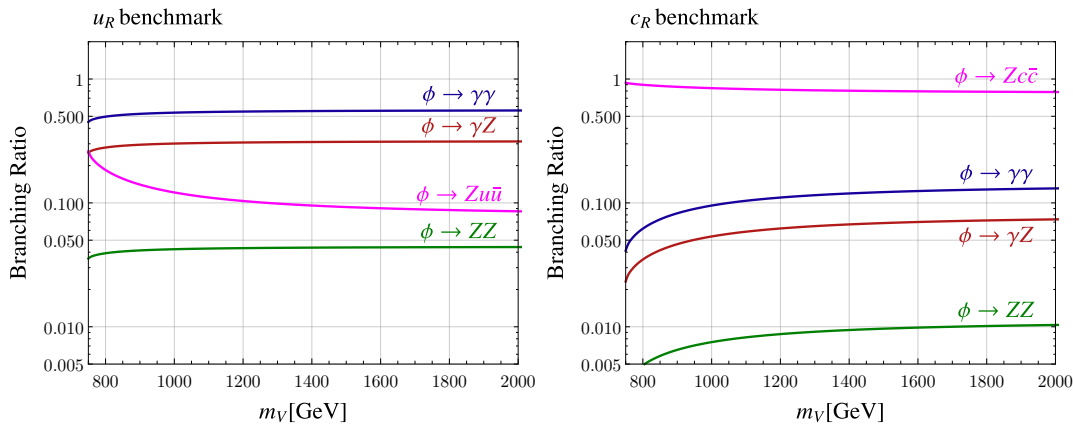


FIG. 2: The different branching ratios for ϕ . The loop-induced decays to $\gamma\gamma$, γZ , and ZZ always compete with the 3-body decay. At large mixing, the 3-body decay is the preferred decay mode, however for small-mixing, the loop-induced decays (which are roughly independent of the mixing) dominate. **Left:** The branching ratios for the u_R benchmark point (small-mixing). **Right:** The branching ratios for the c_R benchmark (large-mixing).

For small mixing, the 3-body ϕ decay is heavily suppressed making the diphoton rate the dominant mode, i.e. $\text{Br}(\phi \rightarrow \gamma\gamma) \approx 1$, independent of y_ϕ or s_θ . In this case, the inclusive cross section scales as

$$\sigma_{\gamma\gamma} \propto y_\phi^2 s_\theta^2 \quad (\text{small mixing}). \quad (18)$$

The transition between the two regimes occurs around $s_\theta \sim 0.2$, and this is the point where the cross section is maximized. Due to the constraints, the up mixing case is always in the small mixing scenario while the charm can be either the large or small mixing regimes. For our chosen benchmark point, the charm scenario corresponds to large mixing.

To reproduce the excess, we simulate the production of ϕ at leading order using a custom FEYNRULES model [25] with MADGRAPH5 [26]. To roughly estimate the size of next-to-leading order (NLO) effects, we compute the production cross section with an additional jet, finding that it makes up about 50% of the leading order cross section. This suggests an NLO K -factor of about 1.5, and we use this correction throughout. We compute the diphoton rate using equation 15 and the branching ratios given in appendix A 2. Figure 3 shows the inclusive diphoton production cross section for different VLQ masses and values of y_ϕ for the two benchmark points.

We see in the left of figure 3 that we need $y_\phi \sim 0.7$ to get enough cross section to explain the excess in the up quark variation of the model. Larger Yukawa couplings are required in the charm-mixing benchmark point, requiring $y_\phi \sim 2$ to achieve the minimum cross section needed to explain the excess.

As with many models explaining the diphoton excess, such Yukawa couplings can lead to non-perturbativity of the model before the GUT scale. The up-mixing benchmark becomes non-perturbative at around 100 TeV, although there is some parameter space where the coupling

remains perturbative beyond the GUT scale. The charm-mixing model is more problematic given the Yukawa coupling runs to its perturbative limit at a few TeV, putting into question the validity of our analysis. However, this problem can be easily overcome by adding additional flavors of bidoublets (these may or may not mix with the SM quarks) which feed into the running, but also boost the diphoton decay rate as the square of the number of flavors allowing for much smaller couplings, and a much higher scale of strong coupling.

C. Eliminating tension with 8 TeV data

One of the puzzling features of the 13 TeV diphoton excess is its seemingly large cross section compared to cross section limits from 8 TeV searches. A 750 GeV resonance is not ruled out by Run I searches but, depending on the production mechanism and width, may be in tension with Run I limits [24, 27]. Thus to reproduce the excess, it is important to have sufficiently large scaling, r , defined as the ratio of the cross section at 13 TeV to that at 8 TeV. We compute the scaling for our model as a function of the VLQ mass (the scaling is independent of the couplings) and assuming the K -factor is constant from 8 to 13 TeV. The results are shown in figure 4 alongside the scaling of other proposed models, including gluon fusion, $q\bar{q}$ production [28], and photon fusion [29–31]. The up-mixing model inherits the scaling from the $u\bar{u}$ production at $m_V \sim 750$ GeV but grows with the mass of the VLQ due to the higher center-of-mass energy. For heavy VLQ masses near 1500 GeV, the scaling is comparable to gluon fusion. The charm variation of the model, however, scales much better due to the parton distribution function of the charm in the initial state. For VLQ masses nearly degenerate with m_ϕ ($800 \text{ GeV} \lesssim m_V \lesssim 1000 \text{ GeV}$) for which

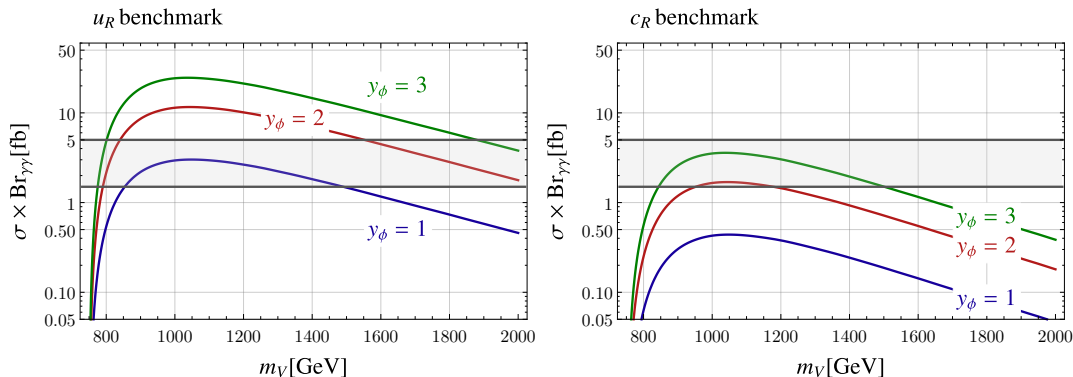


FIG. 3: The inclusive cross section into $\gamma\gamma$ as a function of VLQ mass and varying the values of y_ϕ . In gray we show the rough cross section necessary to explain the excess with a narrow width (1.5 – 5 fb) [24]. **Left:** The cross section for the u_R benchmark point. **Right:** The cross section for the c_R benchmark point.

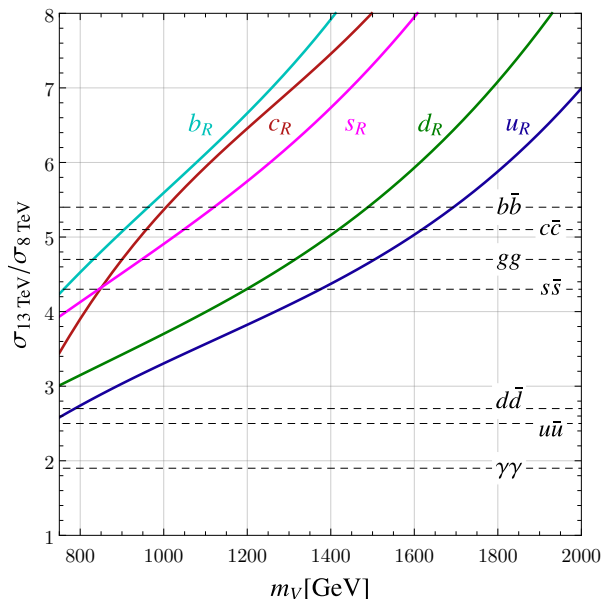


FIG. 4: The ratio of $\sqrt{s} = 13$ to 8 TeV cross section of the up-mixing signal (blue) and charm-mixing signal (red). We have included the scaling properties of the down-type version of this model where the down (green), strange (pink), or bottom (light blue) quark mix with VLQs. The scaling of other proposed production processes are shown as dashed lines and were taken from [3].

the extra jet from the U decay is relatively soft, the scaling is as large as for $b\bar{b}$ production. For larger masses, the charm-mixing scenario has $r \gtrsim 7$, but in this region of parameter space, the ϕ would be accompanied by a high- p_T jet in the final state (we explore the plausibility of this scenario in Sec. IV). We conclude that, depending on the mass of the VLQ, our signal can achieve larger cross section scaling from 8 to 13 TeV than any proposed model of single resonance production.

For simplicity, we have only considered mixing with up-type quarks. It is possible to construct a similar model in which new VLQs mix with the down-type quarks. The terms in the Lagrangian responsible for production of a down-type variation of this model are presented in appendix A 4. We include the scaling properties of production from down, strange, and bottom quark mixing in figure 4. The bottom quark mixing scenario has the largest ratio of 13 to 8 TeV cross section, while the down and strange quark scenarios interpolate between the scaling of the up and charm scenarios.

IV. KINEMATICS

A. Comparing with ATLAS

In addition to the diphoton resonance signature at $m_{\gamma\gamma} \sim 750$ GeV, our signal has two additional jets, with one of the jets typically in the forward direction. ATLAS and CMS have remarked that events in the excess region are consistent with the background kinematics. Furthermore, ATLAS has recently provided kinematic distributions of the excess events [32] for the number of jets, N_{jets} (ATLAS defined a jet using $p_T^j > 25$ GeV for $\eta < 2.4$ and $p_T^j < 50$ GeV for $\eta < 4.4$), and the transverse momentum of the $\gamma\gamma$ resonance, $p_T^{\gamma\gamma}$. Furthermore, ATLAS provided estimates for the expected SM diphoton background from simulations. The distributions are provided for the region $700 \text{ GeV} < m_{\gamma\gamma} < 840 \text{ GeV}$ and with the requirements on the leading and subleading photon energies $E_T^{\gamma 1} > 0.4m_{\gamma\gamma}$ and $E_T^{\gamma 2} > 0.3m_{\gamma\gamma}$. In this bin, ATLAS found a total of 34 events, about 10 of which are diphoton excess candidates.

To compare the compatibility of the kinematics of the excess with our signal we simulate our signal using a combination of MADGRAPH5, PYTHIA 8.2 [33], and DELPHES

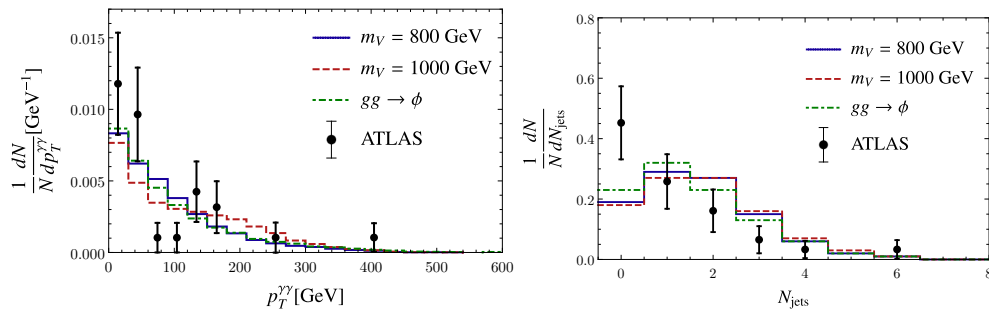


FIG. 5: The kinematic distributions of the sum of the signal and background for vector-like quark mass of 800 (blue) and 1000 GeV (red) compared to the distributions observed by ATLAS (black) with 3.2 fb^{-1} of data. We also provide gluon fusion kinematics (green) for comparison. The N_{jets} and $p_T^{\gamma\gamma}$ distributions for the background and observed events are obtained from the slides presented by ATLAS [32].

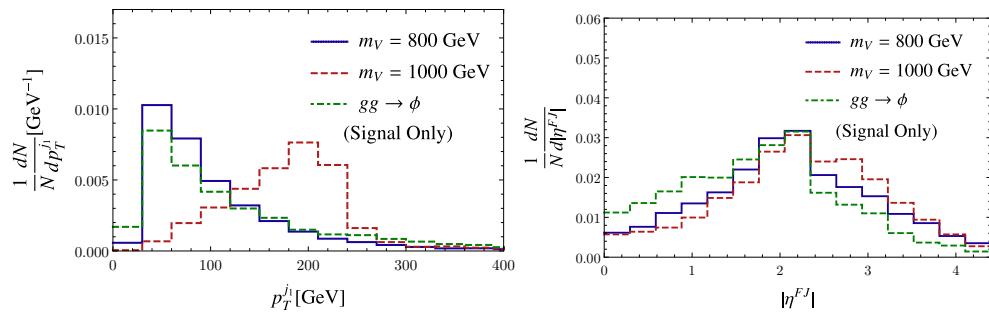


FIG. 6: The leading-jet p_T and forward jet pseudorapidity distributions of the signal for vector-like quark mass of 800 (blue) and 1000 GeV (red) along with a gluon fusion signal (green) for comparison. For VLQs almost degenerate with the resonance, the signal is difficult to differentiate from the QCD background or a resonance produced via gluon fusion since these events also contain soft, forward jets from initial state radiation.

3 [34] making use of the NNPDF2.3LO parton distribution functions [35]. To compare with the distributions observed by ATLAS, we perform a weighted sum of our signal and the background estimates provided by ATLAS

$$N = rN_{\text{sig}} + (1-r)N_{\text{bkg}}. \quad (19)$$

This is done for each bin and we take $r \approx 10/34$. We also simulate gluon fusion at leading order and perform this procedure in order to compare our signal with the kinematics of single production. By comparing the distributions in figure 5, we conclude that although our signal has two extra jets in the final state, the distributions for N_{jets} and $p_T^{\gamma\gamma}$ are consistent with the data provided by ATLAS (as is also the case for the gluon fusion signal). Furthermore, the mass of the VLQ has only a mild effect on these distributions since the number of jets from the hard process is independent of m_V . The signal does have distinctive features in other distributions, however, and we explore these features in the next section.

B. Additional signatures

Our signal predicts observable jet signatures that can be used to discern this process from background events or

from other resonance production mechanisms. In particular, we expect a forward jet as well as one central jet with higher p_T , depending on m_V . The distributions for the p_T of the leading jet ($p_T^{j_1}$) and the absolute value of the pseudorapidity of the most forward jet ($|\eta^{FJ}|$) for the signals with $m_V = 800$ and 1000 GeV are shown in figure 6 along with the gluon fusion signal for comparison. Note that ATLAS and CMS did not provide the background or observed kinematic distributions for these observables, so we did not combine the background and the signal in these plots.

The distributions have some distinctive characteristics. Firstly, we see that for small splitting $p_T^{j_1}$ is peaked around zero since, at these splittings, the central jet, which will typically be the leading jet, has low p_T . However, for larger splitting the distribution has a kinematic edge with the end-point at the splitting between the VLQ and the resonance. This is prototypical of a jet arising from a heavy particle decay to a second heavy particle. Interestingly, such a distribution can suggest the mass of the VLQ. The forward jet in the event is most easily probed using its pseudorapidity. The distribution has a dip at $\eta \approx 2.4$ as a consequence of the cuts used by ATLAS for the jet definition (see above). As expected, the signal has a jet with large η , however this is also true of

the dominant background, $\gamma\gamma$. In this background, jets are emitted from the initial state and hence tend to be in the forward region. This can result in the feature being well hidden inside the SM background of the searches.

In addition to the features of the dominant production mode, there are secondary production modes of the excess. In principle, one may expect that any of the VLQs could decay into the resonance, but this is not the case. Due to the custodial structure of the model, only U couples to the resonance and a SM quark (see equation 10), and hence its the only single VLQ production mode. However, there are three subdominant modes which can contribute significantly to the cross section, single VLQ production through $pp \rightarrow UZ, \bar{U}Z$, QCD pair production of VLQs through $pp \rightarrow U\bar{U}$, and direct production of the resonance through a t -channel VLQ, $pp \rightarrow \phi Z$. The cross section composition depends strongly on the choice of mixing angle and mass of the VLQ. The various contributions to the total cross section as a function of the mass for our benchmark points are shown at leading order in figure 7 (for simplicity we do not apply K -factors when comparing between these different channels). We conclude that the additional production modes make up 10-30% of the inclusive diphoton cross section for reasonable choices of parameters. With more statistics, excesses in these subleading channels could be used to differentiate our signal.

Lastly we note that in principle the charged scalars, which are almost degenerate with ϕ , can also be observed as they are singly produced by a similar mechanism as ϕ . However, the loop-induced decays to WZ and $W\gamma$ both vanish in the custodial limit, rendering their 3-body decays dominant in almost all of parameter space. These 3-body decays could be probed, but such studies are likely less sensitive than other searches.

V. CONCLUSIONS

We have presented a model describing a 750 GeV diphoton resonance arising from a custodial triplet which is produced as a decay product of a singly-produced VLQ. Our model has novel kinematics compared to other proposed production mechanisms and eliminates the tension from the 8 TeV diphoton searches while maintaining consistency with the kinematic distributions in the excess region. With additional statistics, our signal could be confirmed by the presence of a forward jet in the diphoton events or as a kinematic edge in the leading-jet p_T distributions if the VLQ mass is significantly heavier than 800 GeV. The scalar resonance enjoys custodial protection, explaining the dominance of the $\gamma\gamma$ decay rate over

WW , hh , and dijet decays.

Additional signatures of the model include a corresponding excess in the $Z\gamma$ and ZZ channels with fixed rates with respect to the $\gamma\gamma$ rate. Furthermore, searches for single production of VLQs in Run II will probe deep into the viable parameter space of this model.

We now note some interesting model building possibilities which we leave for future studies. First, in this work we focus on the case where the new scalar arises from an $SU(2)_R$ triplet but is uncharged under $SU(2)_L$. However, many of the benefits enjoyed by this model are present in similar representation choices, in particular if ϕ is a $(\mathbf{3}, \mathbf{1})$ or $(\mathbf{3}, \mathbf{3})$ under $(SU(2)_L, SU(2)_R)$. These models also forbid gluon fusion and the tree-level production mechanism can dominate. Another interesting possibility is if the VLQs are related to the top sector, as one might expect in a composite Higgs model, and the custodial symmetry is broken explicitly by the top Yukawa. Such a breaking can induce ϕ production through gluon fusion, perhaps in a controlled manner such that the decays to hh as well as decays to W^+W^- are still suppressed. Finally, we comment on some ways to further reduce the size of the Yukawas. In this work we focused on a single flavor of VLQ for simplicity. However, if there are additional flavors (with or without mixing to the other SM quarks), this can greatly enhance the diphoton decay rate, reducing the size of Yukawas necessary to reproduce the excess. An additional possibility is if $SU(2)_R$ is gauged. In this case, the additional gauge bosons will propagate in the diphoton loop giving a significant enhancement to the diphoton rate.

ACKNOWLEDGMENTS

We thank Eric Kuflik for collaboration in the early stages of this project. We are grateful to Kiel Howe and Wee Hao Ng for useful discussions. This work was supported in part by the NSF through grant PHY-1316222. JD is supported in part by the NSERC Grant PGSD3-438393-2013.

Appendix A: Model details

1. Couplings

In this section, we derive the couplings relevant for the model between the quarks and the vector-like quarks, beginning with the Z couplings. The Z boson interactions with the up-type quarks in the interaction basis are given by (we define $\not{Z} \equiv \bar{\sigma}^\mu Z_\mu$)³

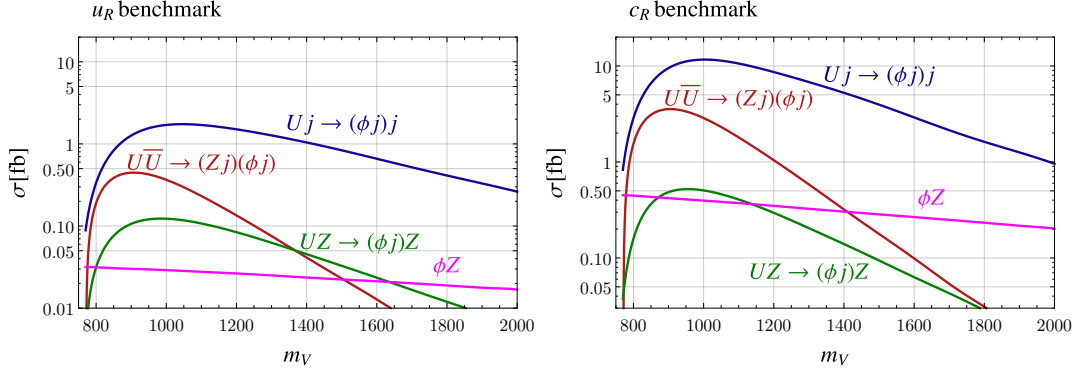


FIG. 7: The cross sections for the different production modes at our benchmark points. We see that production through single VLQ dominates with the secondary production modes providing up to 10-30% corrections on the inclusive diphoton cross section.

$$\mathcal{L}_Z = \frac{e}{c_w s_w} \left\{ \frac{2}{3} s_w^2 \bar{u}^{(0)\dagger} \not{Z} u^{(0)} + \left(\frac{1}{2} + \frac{2}{3} s_w^2 \right) \bar{U}_1^\dagger \not{Z} U_1 + \left(-\frac{1}{2} + \frac{2}{3} s_w^2 \right) \bar{U}_2^\dagger \not{Z} U_2 \right\} \quad (\text{A1})$$

$$= \frac{e}{s_w c_w} \mathbf{u}^{(0)\dagger} \begin{pmatrix} \frac{2}{3} s_w^2 & 0 & 0 \\ 0 & \frac{1}{2} + \frac{2}{3} s_w^2 & 0 \\ 0 & 0 & -\frac{1}{2} + \frac{2}{3} s_w^2 \end{pmatrix} \not{Z} \mathbf{u}^{(0)}, \quad \mathbf{u}^{(0)} \equiv \begin{pmatrix} \bar{u}^{(0)} \\ \bar{U}_1 \\ \bar{U}_2 \end{pmatrix}. \quad (\text{A2})$$

Notice that we can split the coupling matrix into two pieces,

$$\frac{2}{3} s_w^2 \begin{pmatrix} 1 & 0 & 0 \\ 0 & 1 & 0 \\ 0 & 0 & 1 \end{pmatrix} + \frac{1}{2} \begin{pmatrix} 0 & 0 & 0 \\ 0 & 1 & 0 \\ 0 & 0 & -1 \end{pmatrix}. \quad (\text{A3})$$

The first matrix is diagonal and commutes with the rotation to the mass basis while the second matrix yields new couplings between the VLQs and the quarks upon moving to the mass basis. Performing the rotation (the rotation matrices are given in eq. 4) gives,

$$\mathcal{L}_Z = \frac{e}{c_w s_w} \left\{ \frac{1}{2} \mathbf{u}^\dagger \begin{pmatrix} 0 & 0 & -s_\theta \\ 0 & 0 & -c_\theta \\ -s_\theta & -c_\theta & 0 \end{pmatrix} \not{Z} \mathbf{u} + \frac{2}{3} s_w^2 \mathbf{u}^\dagger \not{Z} \mathbf{u} \right\}, \quad (\text{A4})$$

$$\mathbf{u} \equiv \begin{pmatrix} \bar{u} \\ \bar{\tilde{U}} \\ \bar{U} \end{pmatrix}.$$

Notice that the rotation to the mass basis has left the top-left entry of the coupling matrix unchanged. This is very

important as it means the mixing with the VLQs does not affect the $Z\bar{u}u$ coupling which is tightly constrained experimentally. We see that we have a new coupling between the quark and the VLQ:

$$\mathcal{L}_{ZuU} = -\frac{e}{c_w s_w} \frac{1}{2} s_\theta (\bar{u}^\dagger \not{Z} U) + h.c. \quad (\text{A5})$$

Now consider the W -boson couplings. The right-handed up quark does not couple to the W in the gauge basis, so the relevant couplings are simply:

$$\mathcal{L}_W = -\frac{g}{\sqrt{2}} \left(\bar{U}_1^\dagger W^- \bar{D} + \bar{X}^\dagger W^- \bar{U}_2 \right) + h.c. \quad (\text{A6})$$

$$\subset -\frac{g s_\theta}{2} \left(\bar{u}^\dagger W^- \bar{D} + \bar{X}^\dagger W^- \bar{u} \right) + h.c. \quad (\text{A7})$$

where we moved to the mass basis in the last line.

2. Decay rates

In this section, we present formulae for the different decay rates used in the text for both the scalar resonance and the U quark.

a. ϕ decays

We begin by considering the tree-level decays of ϕ . The

³ Note that U_1 is the upper component of an $SU(2)_L$ doublet, while U_2 is the lower component of a second doublet.

dominant contribution is

$$\Gamma(\phi \rightarrow Z u \bar{u}) = \frac{m_\phi N_c}{4(4\pi)^3} \frac{m_Q^2}{v^2} s_\theta^4 y_\phi^2 g_Z(\tau) \quad (\text{A8})$$

where N_c is the number of colors, $\tau \equiv m_Q/m_\phi$, and

$$g_Z(\tau) \equiv \int_0^1 dx \int_{1-x}^1 d\bar{x} \frac{(1-x)(1-\bar{x})(2-x-\bar{x}-2\tau^2)^2}{(1-x-\tau^2)^2(1-\bar{x}-\tau^2)^2}. \quad (\text{A9})$$

The other conceivable 3-body decays, $\phi \rightarrow hu\bar{u}$, $\phi \rightarrow Wd\bar{u}$, and $\phi \rightarrow Wu\bar{d}$ vanish identically due to the custodial production.

In addition ϕ has several loop induced decays to vector bosons as well as the Higgs. All the loop induced decays violate custodial symmetry. This can easily be seen at the operator level, where the terms

$$\Phi B_{\mu\nu} B^{\mu\nu}, \quad \Phi W_{\mu\nu}^a W_a^{\mu\nu}, \quad \text{and} \quad \Phi G_A^{\mu\nu} G_{\mu\nu}^A \quad (\text{A10})$$

(where $B_{\mu\nu}, W_{\mu\nu}^a$, and $G_{\mu\nu}^A$ represent the hypercharge, $SU(2)_L$, and QCD field strength tensors respectively) all violate custodial symmetry and $\text{Tr}[\mathcal{H}^\dagger \Phi \mathcal{H}]$ vanishes identically. There is a large breaking of this symmetry from gauging hypercharge, which induces decays into $\gamma\gamma$, γZ , and ZZ . Since gauging hypercharge only breaks $SU(2)_R$, the Z interactions are suppressed by powers of the Weinberg angle, resulting in these being generically subdominant to the photon decays. The general computation of these decay rates is made complicated due to the mixing of the VLQs with the up quark, however since these contributions are suppressed by powers of the mixing angle they are generically small. We have checked the size of these corrections by computing the rates numerically using FEYNARTS3, FORMCALC8, and LOOP-TOOLS2 [36, 37] and we find that the effect is at most 10% in the interesting region of parameter space (though often much smaller), and we neglect these effects for simplicity.

The decay rate of a scalar into two photons mediated by VLQs with mass m_i is [38]

$$\Gamma(\phi \rightarrow \gamma\gamma) = \frac{m_\phi^3 N_c^2}{4(4\pi)^5} e^4 \left(\sum_i \frac{y_\phi^i}{m_i} Q_i^2 A_{1/2}(x_i) \right)^2, \quad (\text{A11})$$

where $x_i \equiv 4m_i^2/m_\phi^2$ and (for $m_i > m_\phi/2$) $A_{1/2}(x) = 2x(1 + (1-x)\arcsin(1/\sqrt{x})^2)$. The sum runs over all VLQs and for a bidoublet the sum is

$$\sum_i \frac{y_\phi^i}{m_i} Q_i^2 A_{1/2}(x_i) = \left[\frac{y_\phi}{m_V} \frac{8}{3} \right] A_{1/2}(x_V), \quad (\text{A12})$$

where the only non-zero contribution arises from the D and X quarks.

The decay to two gluons mediated by VLQs is

$$\Gamma(\phi \rightarrow gg) = \frac{m_\phi^3}{2(4\pi)^5} g_s^4 \left(\sum_i \frac{y_\phi^i}{m_i} A_{1/2}(x_i) \right)^2, \quad (\text{A13})$$

where g_s is the strong coupling constant. For a bidoublet of VLQs with a triplet scalar, the sum is equal to zero showing that gluon fusion is custodially protected as expected.

The decay to ZZ mediated by VLQs is

$$\Gamma(\phi \rightarrow ZZ) = \frac{m_\phi^3 N_c^2}{4(4\pi)^5} \frac{e^4}{s_w^4 c_w^4} \left(\sum_i \frac{y_\phi^i}{m_i} A_{1/2}(x_i) (T_3^i - Q_i s_w^2) \right)^2. \quad (\text{A14})$$

The sum for the bidoublet is:

$$\sum_i \frac{y_\phi^i}{m_i^2} A_{1/2}(x_i) (T_3^i - Q_i s_w^2)^2 = \left[\frac{y_\phi}{m_V} \frac{8}{3} s_w^4 \right] A_{1/2}(x_V). \quad (\text{A15})$$

The decay to $Z\gamma$ is

$$\Gamma(\phi \rightarrow Z\gamma) = \frac{8m_\phi^3 N_c^2}{(4\pi)^5} \frac{e^4}{s_w^2 c_w^2} \left(\sum_i \frac{y_i (T_3^i - Q_i s_w^2) Q_i}{m_i} \times (I_1(x_i, \lambda_i) - I_2(x_i, \lambda_i)) \right)^2 \quad (\text{A16})$$

where $\lambda_i \equiv 4m_i^2/m_Z^2$ and

$$I_1(a, b) \equiv \frac{ab}{2(a-b)} + \frac{a^2 b^2}{2(a-b)^2} [f(a)^2 - f(b)^2] + \frac{a^2 b}{(a-b)^2} [g(a) - g(b)], \quad (\text{A17})$$

$$I_2(a, b) \equiv -\frac{ab}{2(a-b)} [f(a)^2 - f(b)^2], \quad (\text{A18})$$

and $f(x) \equiv \sin^{-1}(1/\sqrt{x})$ and $g(x) \equiv \sqrt{x-1}f(x)$. For the bidoublet,

$$\sum_i \frac{y_i}{m_i} Q_i (T_3^i - Q_i s_w^2) (I_1(x_i, \lambda_i) - I_2(x_i, \lambda_i)) = - \left[\frac{y_\phi}{m_i} \frac{8}{3} s_w^2 \right] (I_1(x_V, \lambda_V) - I_2(x_V, \lambda_V)). \quad (\text{A19})$$

The $\Phi \rightarrow \gamma\gamma$, $Z\gamma$, ZZ decays obey the expected relationship when they all arise from $\Phi B_{\mu\nu} B^{\mu\nu}$:

$$1 : 2 \tan^2 \theta_w : \tan^4 \theta_w \quad (\text{A20})$$

The decay of ϕ to W^+W^- is

$$\Gamma(\phi \rightarrow W^+W^-) = \frac{m_\phi^3 N_c^2}{(4\pi)^5} \frac{e^4}{s_w^4} \left(\sum_i \frac{y_\phi^i}{m_i} A_{1/2}(x_i) \right)^2. \quad (\text{A21})$$

For a bidoublet the sum vanishes identically as expected.

Lastly, the ϕhh operator vanishes at tree-level and at one-loop by custodial symmetry but will be generated at two-loops by custodial symmetry breaking.

b. U^- decays

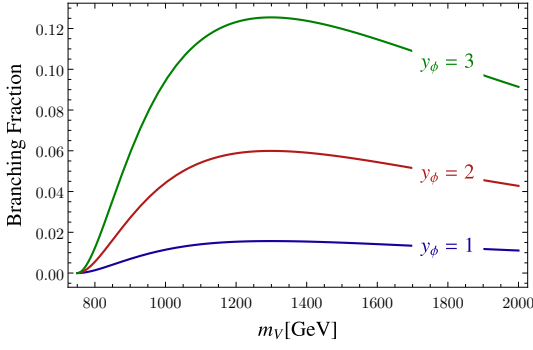


FIG. 8: Branching ratio of the $U \rightarrow u\phi$ decay for different value of the couplings. The fraction is independent of the mixing angle.

The vector-like quarks can decay in a couple ways. We will assume $m_Q > m_\phi$ such that the VLQs can decay to the scalar. Furthermore, we will focus on U since that's the only VLQ that will play a role in the phenomenology.

The decays rates are

$$\Gamma(U \rightarrow uZ) \approx \frac{m_V}{64\pi} \frac{e^2 s_\theta^2}{s_w c_w} \frac{m_V^2}{m_Z^2} \quad (\text{A22})$$

$$\Gamma(U \rightarrow u\phi) = \frac{m_V}{32\pi} y_\phi^2 s_\theta^2 \left(1 - \frac{M_\phi^2}{m_V^2}\right)^2 \quad (\text{A23})$$

Notice that the uZ decay is enhanced by m_V^2/m_Z^2 due to the longitudinal polarization of the Z . Thus in order for the ϕ decay to be substantial one needs larger Yukawas. The branching ratio into ϕu is shown in figure 8 for different Yukawas.

3. Custodial symmetry breaking

In this work we have assumed that the couplings and masses of the VLQs and the triplet Φ preserve the custodial symmetry, which enforces a cancellation in the loop amplitudes corresponding to the gluon fusion production of ϕ as well as the decays to gg , hh , and WW . Assuming no cancellations or large mass hierarchies, a generic scalar ϕ coupling to N_f VLQs with coupling y_ϕ would acquire an effective coupling to gluons of the form

$$\mathcal{L}_{\text{generic}} \supset -\frac{1}{16\pi^2} \frac{N_f g_s^2 y_\phi}{4m_\phi} \phi G^{\mu\nu, A} G_{\mu\nu}^A, \quad (\text{A24})$$

with similar expressions for the other amplitudes. The explicit breaking of custodial symmetry due to the gauging of hypercharge means that these amplitudes will still be generated, but with an additional suppression of $\mathcal{O}(\alpha/c_w^2)$ compared to the above estimate.

In particular, the VLQ mass renormalization and the renormalization of the $\text{Tr}[\bar{V}\Phi V]$ couplings due to hypercharge gauge boson loops, illustrated in Figure 9,

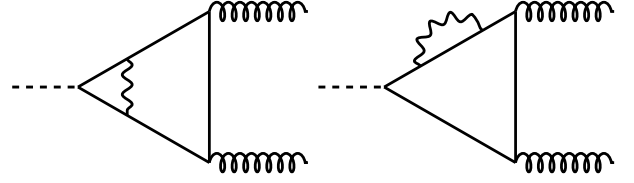


FIG. 9: Prototypical loop contributions to the custodial symmetry breaking amplitudes. Such two-loop contributions can induce gluon fusion production and decays two gluons. Similar diagrams can give rise to decays to W^+W^- and hh .

will contribute operators of the form $\text{Tr}[T_3^R \Phi] G^{\mu\nu, A} G_{\mu\nu}^A$. Since the mass and vertex renormalizations are logarithmically divergent, they require counterterms which are not calculable in the effective theory. Instead, we calculate the size of the IR contributions and take this as an estimate of the overall size of the irreducible contributions.

The mass renormalization of the VLQs introduces a mass splitting between the different T_3^R states of size

$$\begin{aligned} \frac{\delta m_V}{m_V} &\simeq \frac{3g'^2}{16\pi^2} \log\left(\frac{\Lambda^2}{m_V^2}\right) \Delta(Y^2) \quad (\text{A25}) \\ &\simeq \frac{\alpha}{\pi c_w^2} \log\left(\frac{\Lambda^2}{m_V^2}\right). \end{aligned}$$

Similarly, the vertex and wavefunction renormalization provide a contribution to the operator $\delta y_\phi \text{Tr}[\bar{V}T_3^R \Phi V]$ of size

$$\begin{aligned} \frac{\delta y_\phi}{y_\phi} &\simeq \frac{6g'^2}{16\pi^2} \log\left(\frac{\Lambda}{m_V}\right) \Delta(Y^2) \quad (\text{A26}) \\ &\simeq \frac{\alpha}{\pi c_w^2} \log\left(\frac{\Lambda^2}{m_V^2}\right). \end{aligned}$$

where g' is the $U(1)_Y$ coupling constant. Now, custodial symmetry violating amplitudes of the kind in Figure 9 can be generated either with an insertion of δm_V instead of m_V , or with the coupling δy_ϕ . Therefore, the amplitude is suppressed by a factor

$$\frac{\delta \mathcal{A}}{\mathcal{A}_0} \simeq \frac{\delta m_V}{m_V} + \frac{\delta y_\phi}{y_\phi} \quad (\text{A27})$$

$$\simeq \frac{2\alpha}{\pi c_w^2} \log\left(\frac{\Lambda^2}{\text{TeV}^2}\right) \quad (\text{A28})$$

In the same spirit, one can also generate a mixing between the Higgs and the new scalar ϕ . Such a mixing is induced at two loops from the operator of the form, $y_{\Phi HH} m_\phi \text{Tr}[H^\dagger T_3^R \Phi H]$. The coefficient of this operator is of order

$$y_{\Phi HH} \simeq y_\phi \frac{\lambda_V^2}{16\pi^2} \frac{2\alpha}{\pi c_w^2} \log\left(\frac{\Lambda^2}{\text{TeV}^2}\right), \quad (\text{A29})$$

which results in a mixing angle between the Higgs and ϕ of order

$$\simeq \frac{m_V^2 \tan^2 \theta}{\sqrt{2} v m_\phi} \frac{y_\phi}{16\pi^2} \frac{2\alpha}{\pi c_w^2} \log\left(\frac{\Lambda^2}{\text{TeV}^2}\right) \sim \mathcal{O}(10^{-4} - 10^{-5}), \quad (\text{A30})$$

where we have substituted λ_V for the mixing angle. This mixing will induce decays of ϕ to $t\bar{t}$, but due to the smallness of the coupling, we do not expect this decay to be observable in the near future.

4. Down-type model

We now present the down-type model which can have mixing between the SM down-type quarks and the VLQs. The model is identical to the up-type model but assigning the V bidoublet a $U(1)_X$ charge of $-1/3$ (as opposed to $+2/3$). This gives the following fields

$$V = \begin{pmatrix} D_2 & U \\ Y & D_1 \end{pmatrix} \quad \bar{V} = \begin{pmatrix} \bar{D}_2 & \bar{Y} \\ \bar{U} & \bar{D}_1 \end{pmatrix} \quad (\text{A31})$$

where $Q_{D_1} = Q_{D_2} = -1/3$, $Q_U = +2/3$, and $Q_Y = -4/3$. As in the up-mixing case, a mixing is generated between a SM quark and a VLQ through:

$$\mathcal{L}_{VLQ} = m_V \text{Tr} [\bar{V}V] + \lambda_V \text{Tr} [\mathcal{H}^\dagger V] \bar{d}^{(0)} + h.c. \quad (\text{A32})$$

where $\bar{d}^{(0)}$ denotes the down quark in the SM mass basis of the down-type sector. The mixing produces a ZDd coupling resulting in electroweak production of D , which can decay into the diphoton resonance.

Appendix B: Experimental constraints

The LHC has performed searches with significant sensitivity to models with light-quark mixing. The constraints were studied in detail in [14] for both up-quark mixing and charm-quark mixing in the context of a composite model and in [23] for the up-type mixing model. The dominant constraints arise from charged current production of D and X quarks. There are additional constraints from production of the charged $+2/3$ quarks, but since they are always subdominant, we omit these. Instead of recasting the constraints ourselves we make use of the recast performed in Ref. [14]. The authors recast two searches: a 7 TeV search by ATLAS searching for the bidoublet model (without the additional scalar triplet) [39] and an 8 TeV search for excited quarks [41] with a similar final state which is not optimized for the single production of vector-like-quarks but shares a similar final state. The two searches have competitive limits. Additionally there are constraints on pair production

of VLQs, however these are subdominant in the mass

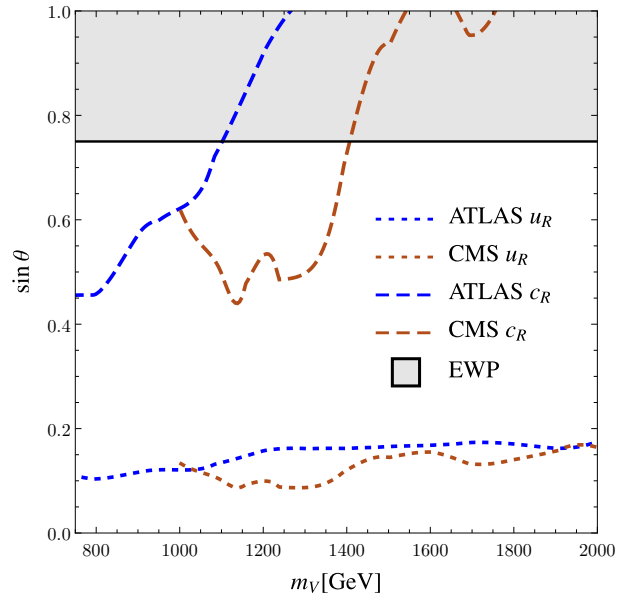


FIG. 10: The constraints on the bidoublet model (reinterpreted from the work of [14]) arising from an ATLAS 7 TeV dedicated search for single production of VLQs [39], a CMS 8 TeV search for W/Z -tagged dijet resonances [40], and electroweak precision (EWP). Areas above the lines are excluded. Here we neglected effects due to additional decay channels of the vector-like-quarks into the scalars in our model.

ranges we are interested in. In particular ATLAS has performed a search for VLQs decaying to Wj finding a limit around 700 GeV for a single VLQ [42]. With two copies of such VLQs the limits strengthen but do not extend past 800 GeV. Furthermore, electroweak precision places an additional constraint from additional contributions to the S parameter [17]. One might worry that the additional scalar would complicate the limits, in particular the VLQs can decay to the scalar weakening the constraints. In general these branching ratios are $\lesssim 10\%$ and we ignore such effects in our discussion.

Our goal is now to convert the single production limits quoted Ref. [14] into our (closely related) framework. In Ref. [14] the authors study a bidoublet model but with an additional VLQ singlet which they denote as \tilde{U} . We can decouple the particle to match with our framework. Multiplying their cross sections by the correction factor,

$$s_\theta^2 \left[\cos \frac{v}{f} \sin \left(\tan^{-1} \left(\frac{y_R f}{m_V} \sin \frac{v}{f} \right) \right) \right]^{-2} \quad (\text{B1})$$

with $f = 600$ GeV, $v \simeq 246$ GeV, and $y_R = 1$ gives the cross sections in our case. Employing this procedure we obtain the limits shown in figure 10.

- [1] ATLAS collaboration, *Search for resonances decaying to photon pairs in 3.2 fb^{-1} of pp collisions at $\sqrt{s} = 13 \text{ TeV}$ with the ATLAS detector*, Tech. Rep. ATLAS-CONF-2015-081, CERN, Geneva, Dec, 2015.
- [2] CMS collaboration, *Search for new physics in high mass diphoton events in proton-proton collisions at $\sqrt{s} = 13 \text{ TeV}$* , Tech. Rep. CMS-PAS-EXO-15-004, CERN, Geneva, 2015.
- [3] R. Franceschini, G. F. Giudice, J. F. Kamenik, M. McCullough, A. Pomarol, R. Rattazzi et al., *What is the gamma gamma resonance at 750 GeV ?*, 1512.04933.
- [4] S. Knapen, T. Melia, M. Papucci and K. Zurek, *Rays of light from the LHC*, 1512.04928.
- [5] X.-F. Han, L. Wang, L. Wu, J. M. Yang and M. Zhang, *Explaining 750 GeV diphoton excess from top/bottom partner cascade decay in two-Higgs-doublet model extension*, 1601.00534.
- [6] F. P. Huang, C. S. Li, Z. L. Liu and Y. Wang, *750 GeV Diphoton Excess from Cascade Decay*, 1512.06732.
- [7] J. Liu, X.-P. Wang and W. Xue, *LHC diphoton excess from colorful resonances*, 1512.07885.
- [8] A. Berlin, *Diphoton and diboson excesses in a left-right symmetric theory of dark matter*, *Phys. Rev.* **D93** (2016) 055015, [1601.01381].
- [9] J. Bernon, A. Goudelis, S. Kraml, K. Mawatari and D. Sengupta, *Characterising the 750 GeV diphoton excess*, 1603.03421.
- [10] V. De Romeri, J. S. Kim, V. Martin-Lozano, K. Rolbieceki and R. R. de Austri, *Confronting dark matter with the diphoton excess from a parent resonance decay*, 1603.04479.
- [11] P. Agrawal, J. Fan, B. Heidenreich, M. Reece and M. Strassler, *Experimental Considerations Motivated by the Diphoton Excess at the LHC*, 1512.05775.
- [12] A. Kobakhidze, F. Wang, L. Wu, J. M. Yang and M. Zhang, *750 GeV diphoton resonance explained as a heavy scalar in top/bottom seesaw model*, 1512.05585.
- [13] P. S. B. Dev, R. N. Mohapatra and Y. Zhang, *Quark Seesaw, Vectorlike Fermions and Diphoton Excess*, 1512.08507.
- [14] C. Delaunay, T. Flacke, J. Gonzalez-Fraile, S. J. Lee, G. Panico and G. Perez, *Light Non-degenerate Composite Partners at the LHC*, *JHEP* **02** (2014) 055, [1311.2072].
- [15] K. Agashe, R. Contino, L. Da Rold and A. Pomarol, *A Custodial symmetry for $Zb\bar{b}$* , *Phys. Lett.* **B641** (2006) 62–66, [hep-ph/0605341].
- [16] A. Atre, M. Carena, T. Han and J. Santiago, *Heavy Quarks Above the Top at the Tevatron*, *Phys. Rev.* **D79** (2009) 054018, [0806.3966].
- [17] A. Atre, G. Azuelos, M. Carena, T. Han, E. Ozcan, J. Santiago et al., *Model-Independent Searches for New Quarks at the LHC*, *JHEP* **08** (2011) 080, [1102.1987].
- [18] M. Redi and A. Weiler, *Flavor and CP Invariant Composite Higgs Models*, *JHEP* **11** (2011) 108, [1106.6357].
- [19] T. Flacke, J. H. Kim, S. J. Lee and S. H. Lim, *Constraints on composite quark partners from Higgs searches*, *JHEP* **05** (2014) 123, [1312.5316].
- [20] M. Redi, V. Sanz, M. de Vries and A. Weiler, *Strong Signatures of Right-Handed Compositeness*, *JHEP* **08** (2013) 008, [1305.3818].
- [21] N. Vignaroli, *Early discovery of top partners and test of the Higgs nature*, *Phys. Rev.* **D86** (2012) 075017, [1207.0830].
- [22] N. Vignaroli, *Discovering the composite Higgs through the decay of a heavy fermion*, *JHEP* **07** (2012) 158, [1204.0468].
- [23] A. Atre, M. Chala and J. Santiago, *Searches for New Vector Like Quarks: Higgs Channels*, *JHEP* **05** (2013) 099, [1302.0270].
- [24] J. F. Kamenik, B. R. Safdi, Y. Soreq and J. Zupan, *Comments on the diphoton excess: critical reappraisal of effective field theory interpretations*, 1603.06566.
- [25] A. Alloul, N. D. Christensen, C. Degrande, C. Duhr and B. Fuks, *FeynRules 2.0 - A complete toolbox for tree-level phenomenology*, *Comput. Phys. Commun.* **185** (2014) 2250–2300, [1310.1921].
- [26] J. Alwall, R. Frederix, S. Frixione, V. Hirschi, F. Maltoni, O. Mattelaer et al., *The automated computation of tree-level and next-to-leading order differential cross sections, and their matching to parton shower simulations*, *JHEP* **07** (2014) 079, [1405.0301].
- [27] A. Falkowski, O. Slone and T. Volansky, *Phenomenology of a 750 GeV Singlet*, *JHEP* **02** (2016) 152, [1512.05777].
- [28] J. Gao, H. Zhang and H. X. Zhu, *Diphoton excess at 750 GeV : gluon-gluon fusion or quark-antiquark annihilation?*, 1512.08478.
- [29] C. Csáki, J. Hubisz and J. Terning, *Minimal model of a diphoton resonance: Production without gluon couplings*, *Phys. Rev.* **D93** (2016) 035002, [1512.05776].
- [30] S. Fichet, G. von Gersdorff and C. Royon, *Scattering Light by Light at 750 GeV at the LHC*, 1512.05751.
- [31] C. Csaki, J. Hubisz, S. Lombardo and J. Terning, *Gluon vs. Photon Production of a 750 GeV Diphoton Resonance*, 1601.00638.
- [32] ATLAS collaboration, “Diphoton searches in ATLAS.” Rencontres de Moriond, 2016.
- [33] T. Sjostrand, S. Mrenna and P. Z. Skands, *A Brief Introduction to PYTHIA 8.1*, *Comput. Phys. Commun.* **178** (2008) 852–867, [0710.3820].
- [34] DELPHES 3 collaboration, J. de Favereau, C. Delaere, P. Demin, A. Giammanco, V. Lemaître, A. Mertens et al., *DELPHES 3, A modular framework for fast simulation of a generic collider experiment*, *JHEP* **02** (2014) 057, [1307.6346].
- [35] R. D. Ball et al., *Parton distributions with LHC data*, *Nucl. Phys.* **B867** (2013) 244–289, [1207.1303].
- [36] T. Hahn and M. Perez-Victoria, *Automatized one loop calculations in four-dimensions and D-dimensions*, *Comput. Phys. Commun.* **118** (1999) 153–165, [hep-ph/9807565].
- [37] T. Hahn, *Generating Feynman diagrams and amplitudes with FeynArts 3*, *Comput. Phys. Commun.* **140** (2001) 418–431, [hep-ph/0012260].
- [38] J. F. Gunion, H. E. Haber, G. L. Kane and S. Dawson, *The Higgs Hunter’s Guide*, *Front. Phys.* **80** (2000) 1–448.
- [39] ATLAS collaboration, *Search for Single Production of Vector-like Quarks Coupling to Light Generations in 4.64 fb^{-1} of Data at $\sqrt{s} = 7 \text{ TeV}$* , .

- [40] CMS collaboration, *Search for heavy resonances in the W/Z -tagged dijet mass spectrum in pp collisions at 8 TeV*, Tech. Rep. CMS-PAS-EXO-12-024, CERN, Geneva, 2013.
- [41] CMS collaboration, CMS, *Search for heavy resonances in the W/Z -tagged dijet mass spectrum in pp collisions at 8 TeV*, .
- [42] ATLAS collaboration, G. Aad et al., *Search for pair production of a new heavy quark that decays into a W boson and a light quark in pp collisions at $\sqrt{s} = 8$ TeV with the ATLAS detector*, *Phys. Rev.* **D92** (2015) 112007, [1509.04261].